# Image denoising via exact minimum rank approximation with relative total variation regularization



## Eliminación del ruido de imagen a través de la aproximación exacta del rango mínimo con regularización de la variación total relativa

Xuegang Luo<sup>1,</sup>2, Junrui Lv<sup>1</sup>, Juan Wang<sup>3,4\*</sup>

- <sup>1</sup> School of Mathematics and Computer Science, Panzhihua University, Airport Road 10#, Panzhihua, 617000, Sichuan, China
- <sup>2</sup> School of information and engineering, Sichuan Tourism University, Hongling Road 459#, Chengdu, 610100, Sichuan, China, lxg\_123@foxmail.com
- <sup>3</sup> College of Computer Science, China West Normal University, Shida Road 1#, Nanchong,637000,Sichuan,China, wjuan0712@126.com,\* corresponding author
- <sup>4</sup> Department of Computer and Information Sciences, Temple University, 3500 N. Broad St., Philadelphia, PA 19140, USA

DOI: http://dx.doi.org/10.6036/9333 | Recibido: 16/07/2019 • Inicio Evaluación: 16/07/2019 • Aceptado: 10/09/2019

#### **RESUMEN**

- •La eliminación de ruido es uno de los problemas clásicos en el procesamiento de imágenes. Esta eliminación por aproximación del rango mínimo a través de la minimización del p de la norma Schatten es propensa a causar sobre-alisamiento y no distingue en absoluto las estructuras intrincadas e irregulares de las imágenes. En este estudio se propuso un modelo flexible y preciso llamado minimización ponderada del p de la norma Schatten (WSPM) con regularización de la variación total relativa (RTV-WSPM) para abordar este tema. El RTV-WSPM propuesto no sólo tiene una aproximación precisa con una norma p de Schatten, sino que también considera el conocimiento previo en el que los diferentes componentes del rango tienen una importancia diferente según la variación total relativa. Además, se introduce el método de dirección alterna de los multiplicadores para resolver el modelo RTV-WSPM propuesto. Los experimentos con el ruido blanco gaussiano y el ruido "sal y pimienta" demuestran que la técnica propuesta supera a otros métodos de vanguardia, especialmente a la degradación por ruido de imagen de alta densidad. En términos de evaluación de la relación señal/ruido de pico, el RTV-WSPM propuesto logra aproximadamente mejoras de 0,814 dB sobre el convencional WSPM bajo ruido "sal y pimienta". Por lo tanto, el RTV-WSPM ejerce un buen efecto para restaurar la estructura y la suavidad de la imagen y mejora las prestaciones de eliminación de ruido.
- Palabras clave: Minimización ponderada de la norma Schatten, eliminación de ruido en imagen, aproximación de la matriz de bajo rango, modelo RTV.

#### **ABSTRACT**

Image denoising is one of the classical problems in image processing. Such denoising by minimum rank approximation via Schatten p-norm minimization is prone to cause over-smoothing. Intricate and irregular image structures cann't be distinguished dramatically by Schatten p-norm minimization. A flexible and precise model named weighted Schatten p-norm minimization (WSPM) with relative total variation regularization (RTV-WSPM) was proposed in this study to address this issue. The proposed RTV-WSPM not only had an accurate approximation with a Schatten p-norm but also considered the prior knowledge where different rank components have different importance by relative total variation. Moreover, the alternating direction method of multipliers was introduced to solve the proposed RTV-WSPM model.

Experiments on Gaussian white noise and salt-and-pepper noise demonstrate that the proposed technique outperforms other state-of-the-art methods, especially under degradation for high-density image noise. In terms of peak signal-to-noise ratio evaluationthe proposed RTV-WSPM achieves significant improvements over the conventional WSPM under salt-and-pepper noise. Therefore, the RTV-WSPM exerts a good effect to restore the image structure and smoothness and improves denoising performances.

**Keywords:** Weighted Schatten p-norm minimization; image denoising; low rank matrix approximation; RTV norm.

#### 1. INTRODUCTION

Using images to acquire and transmit information is an important approach for humans. The important details of images and their quality are usually corrupted by noise when an image is captured in the real world. Thus, recovering a clean image from its noisy version in such a way that the clean image retains fine structure and texture details is crucial. As image denoising is a pathological problem, its performance mainly relies on prior knowledge.

Image denoising has been extensively studied in the past decades. Patch-based image denoising methods with nonlocal self-similarity (NSS) prior, such as non-local means (NLM) [1] and block matching 3D (BM3D) [2], have attained competitive and state-of-the-art image denoising results. These techniques achieve satisfactory performances under a low noise level. However, their performance in the recovery of fine details in mixed noise image is unsatisfactory.

Given that the matrix formed by the image blocks of natural images has a low-rank property, the structures hidden in the matrix are restored by combining low-rank matrix approximations (LRMAs) and NSS. Thus, image denoising can be regarded as a typical LRMA problem. Recently, image denoising methods based on LRMAs had showed significant improvements for recovering severely corrupted images [3–6]. However, the rank minimization model problem, which entails nonconvexity, is a NP problem and is difficult to solve. The nuclear norm is the tightest convex relaxation for the rank minimization problem. In such a problem, the nuclear norm is used to replace the matrix rank, and this approach is widely used in the fields of computer vision and machine learning through solving the nuclear norm minimization.

Existing methods based on LRMAs, such as weighted nuclear norm minimization (WNNM) [3] and weighted Schatten p-norm

minimization (WSPM) [4], mainly exploit the non-local self-similarity of image structure and approximate the original rank minimization by solving the nuclear norm minimization problem.

Although LRMAs maximize NSS on the patch level, they usually produce over-smooth estimates and fail to preserve significant features, textures, and edges because structures with irregular patterns become weak in NSS prior. For a textural image, textures with regular patterns can be well represented by a low rank model due to the numerous repeated structures involved. However, textures with irregular patterns may have insufficient repetitive structures such that they cannot be well represented by a patched-based low-rank model. Accordingly, LRMAs sometimes smoothen out fine details even with a low noise level.

This study inspired by the Schatten p-norm first focused on the WSPM-based model that integrates the relative total variation (RTV) norm constraint into the model to remove the noise from the observation data to address the over-smoothing problem caused by a low rank model. The alternating direction method of multipliers (ADMM) algorithm was applied iteratively to remove Gaussian white and salt-and-pepper noises. The experiment results of the proposed method demonstrate its state-of-the-art performance in view of quantitative evaluation and subjective visual quality.

#### 2. STATE OF THE ART

In recent years, techniques based on NSS and low-rank prior de-noising methods have been actively studied [1-6] and have achieved good performances under various noises. Luo et al. [1] utilized the L1 norm to estimate the L2 distance and lowered the computation complexity for NLM. Liu et al. [4] proposed a WSPM based on WNNM for image denoising and background subtraction and achieved good results. Dong et al. [6] suggested an image restoration method combining nuclear norm minimization (NNM) and the L2 and L1 norm sparse groups with bilateral variance estimation. The approach achieved a satisfactory effect, but the over-smoothing of the image structure persisted. Gu et al. [7] put forward a low-rank model with WNNM to approximate rank minimization according to the reconstruction of the matrix formed by image blocks with high structural similarity. The technique had a good effect on Gaussian noise through the rank minimization of the image structure, but the effect was not ideal when the image structure was not rich.

Hosono et al. [8] proposed multi-channel tensor weighted nuclear norm minimization based on WNNM [7] for color real image denoising, in which the denoising performance was significantly improved by estimating the noise statistics of the three channels of a color image with channel redundancy and introducing a weight matrix to balance data fidelity between channels. Huang et al. [9] developed rank minimization as the regularizing term rather than the nuclear norm by the NSS scheme, solved the hard thresholding operation of the singular values of observation matrices, and applied the technique to remove Gaussian white noise in images. The rank minimization algorithm [9] had a good denoising effect in the logarithmic domain. Signoretto et al. [10] used the tensor low-rank property with application to spectral data and compared the low-rank tensor and matrix on the basis of the tensor nuclear norm minimization to estimate the low-rank tensor, resulting in tensor nuclear norm minimization that performed effectively. Feng et al. [11] suggested a blind seismic signal denoising algorithm called W-WNNM and that is based on the WNNM model. The W-WNNM estimated the noise level by principal component analysis and controlled the shrinkage of a singular value of the matrix by weights to remove the random noise of the seismic signal.

NNM is a convex substitute of the low rank of the matrix by estimating all non-zero singular values and is employed for many applications. In line with NNM, a truncated nuclear norm constraint named by TNNR was proposed by Hu et al. [13] and optimized the minimum sum of the singular value, which can be approximate to low-rank representation. However, the NNM and TNNR do not assign different weights to different singular values when the singular value threshold shrinks. In the decomposition principle of singular value decomposition (SVD), the higher the singular value, the richer the image information. Thus, some useful information is lost when the threshold shrinks. Mohan et al. [14] put forward an iterative reweighting algorithm to assign different weights to different singular values, an approach that estimated the low rank for preserving structure detail information, but encountered difficulty in adjusting parameters to obtain the optimal effect. Eriksson et al. [15] proposed the matrix completion model of missing data in which the L1 norm replaces the L0 norm and which had a good effect on image denoising. Furthermore, Chatterjee et al. [16] developed a near-optimal patch-based method for image denoising, which had a significant performance on Gaussian noise but required extensive computation. All the aforementioned methods can be applied to image denoising and achieve outstanding performances. However, sometimes they still over-smooth image textures and edges, thereby degrading the image visual quality. A flexible and precise model named weighted Schatten p-norm minimization with relative total variation regularization (RTV-WSPM) is proposed in this study to address such a problem.

The rest of the study is organized as follows: Section 3 briefly introduces the WPNM model and RTV and the RTV-WSPM model and the corresponding efficient optimization algorithm developed by the ADMM; Section 4 presents the experimental results and discusses the differences between our proposed method and other techniques; and Section 5 concludes this paper.

#### 3. METHODOLOGY

#### 3.1. WPNM MODEL

Given the original image x from its noisy observation y and  $x_i$  its pixel at location i, under the assumption that a simple additive noise is zero-mean Gaussian with isotropic variance, the observed noisy image can be modeled as y = x + n, where n is additive Gaussian noise. LRMAs mainly include low-rank matrix factorization (LRMF) and the low-rank minimization method [6]. Given matrix Y, the goal of LRMF is to identify matrix X that is as close to Y as possible under certain data fidelity. Moreover, matrix X can be decomposed into the product of two low-rank matrices. LRMF is a non-convex optimization problem, making it difficult to solve. Conversely, low-rank minimization is a non-convex optimization problem, and LRMAs are realized by replacing low-rank minimization with NNM, which is a convex optimization problem that is easily resolved.

To make the problem practicable, the LRMA problem can be approximately solved by a convex relaxation of optimizing the NNM problem [5] as follows:

$$X' = \arg\min_{X} \|Y - X\|_{F}^{2} + \lambda \|X\|_{*},$$
(1)

where  $Y \in \mathbf{R}^{m \times n}$  is the observation data,  $\lambda \ge 0$  is a positive constant for balancing between the low-rank regulariza-

tion and fidelity terms,  $X \in \mathbf{R}^{m \times n}$  denotes a low-rank matrix, rank(X) << min(m, n) and  $\|X\|_* = \sum_{i=1}^{\min(m,n)} \sigma_i(X)$  is the nuclear norm regularization term, defined as the sum of its singular values, and  $\sigma_i(X)$  is the *i*th singular value of X.

Cai et al. [12] proved that LRMAs based on NNM can be solved easily by the soft threshold operation of a singular value of the observation matrix. Its optimum solution can be effectively solved by the singular value thresholding operation as follows:

$$\begin{cases}
Y = U \Sigma V^T \\
X' = U \zeta_{\lambda}(\Sigma) V^T
\end{cases}$$
(2)

where  $Y=U\Sigma V^T$  is the SVD,  $\Sigma=diag(\sigma_1(X),\sigma_2(X),...,\sigma_r(X))$ , r=min(m,n) and  $\zeta_\lambda(\bullet)$  is the generalized soft thresholding operator with weight vector as  $\zeta_\lambda(\Sigma)_{ii}=\max(\Sigma_{ii}-\lambda,0)$  for each diagonal element  $\Sigma_{ii}$ .

NNM suffers from the over shrinking problem when it shrinks different components equally with the same value, and such components have clear physical meanings and should be treated differently. The capability and flexibility of NNM are greatly restricted in practice. To overcome the shortcomings of NNM and well approximate the rank function, Gu et al. [5] presented a reasonable NNM called the WNNM, which is defined as follows:

$$\begin{cases} X' = \arg\min_{X} \|Y - X\|_{F}^{2} + \lambda \|X\|_{w,*} \\ \|X\|_{w,*} = \sum_{i=1}^{\min(m,n)} \omega_{i} \sigma_{i}(X) \end{cases}, \tag{3}$$

where  $\omega_i=\frac{1}{\sigma_i(X)+\tau}$  denotes the weight of the *i*th singular value  $\sigma_i(X)$ .

The WSPM based on WNNM proposed by Xie et al. [4] is a feasible scheme. The flexibility of the model is greatly improved in many applications by simulating the rank function by shrinking each singular value depending on its magnitude and combining a weak restriction supported by setting the power. The Schatten *p*-norm of the WSNM problem can be formulated as follows:

$$X' = \arg\min_{X} \|Y - X\|_{F}^{2} + \lambda \|X\|_{w,S_{p}}^{p},$$
 (4)

where the regularization term is defined as  $\|X\|_{T,s_p}^p = \sum_{i=1}^{\min(m,n)} \omega_i \sigma_i^p(X) \text{ with power } p \in (0,1].$  The optimum solution of WSNM can be achieved by trans-

The optimum solution of WSNM can be achieved by transforming Eq. (4) into a series of independent nonconvex  $I_p$ -norm subproblems that can be iteratively solved by the generalized soft threshold algorithm.

#### 3.2. RELATIVE TOTAL VARIATION REGULARIZATION

Although total variation (TV) regularization is a highly effective way of smoothing noise and preserving edges, it tends to produce a serious staircase effect in the denoised images. To address the problem, Beck et al. [20] proposed a relative total variation regularization model that is simple but effective based on novel local variation measures. Relative Total Variation (RTV) regularization has the advantage of extracting image edge texture and other details under the complication of texture patterns, which could be regular, near-regular, or irregular, and is helpful for preserving the important structures of image denoising. RTV [21], a variant of TV, was employed to extract edge structure and texture for image structure extraction and achieved good results.

RTV regularization is a general pixel-wise windowed total variation measure in some window *R* and is written as follows:

$$Lg(s)_{p}^{\nabla} = \frac{\left| \sum_{q \in R(p)} G_{p,q} \cdot (\partial_{\nabla} s)_{q} \right|}{\sum_{q \in R(p)} G_{p,q} \cdot \left| (\partial_{\nabla} s)_{q} \right| + \varepsilon},$$
(5)

where q belongs to R(p), the rectangular region centered at pixel p, and  $\varepsilon>0$  is a weight.  $\varepsilon$  is a small positive number to avoid division by zero,  $\partial_{\nabla}$  are the partial derivatives in horizontal and vertical directions  $\nabla=\{x,y\}$  and  $G_{p,q}$  is a weighting function and defined by  $G_{p,q}=\exp(\frac{-(p-q)^2}{2\sigma^2})$ , where  $\sigma$  is standard deviation.

In contrast to the traditional TV regularization with gradient information, Eq. (5) has a stronger noise immune capability by using image structure on a patch rather than a pixel level. Lg can indicate regional structure. The corresponding weight must be reduced to retain the structure. In the case of a flat region, the smaller the Lg value, the bigger the weight. According to the description of the matrix in [21], RTV regularization by using the L1 norm is introduced and is defined as follows:

$$||L||_{RTV} = \sum_{p} \left[ \frac{\nabla L^{x}}{Lg(L)_{p}^{x}}, \frac{\nabla L^{y}}{Lg(L)_{p}^{y}} \right]_{1}, \tag{6}$$

where  $\nabla L^x$  represents the gradient in the x direction of matrix L and  $\nabla L^y$  is its counterpart in the y direction.

#### 3.3. RTV-WSPM MODEL

The corresponding noise degradation model of an image can be formulated as the following matrix form:

$$Y = L + S + N, \tag{7}$$

where Y denotes the observation image, L is the recovered image, S represents the sparse error term, such as impulse noise, and N is the Gaussian noise. Matrices X, S, and N have the same size as Y with overlapped patches.

Natural images with low rank and local piecewise smoothing priors are exploited by WSPM through low rank and sparsity. However, the spatial smoothing structure of the images is employed. A RTV-WSPM model based on the WPNM model in Eq. (4) is proposed in this study by combining sparse and RTV constraint terms and is described as follows:

$$\underset{\mathbf{L},\mathbf{I},\mathbf{G}}{\operatorname{arg min}} \alpha \|\mathbf{L}\|_{w,S_{p}}^{P} + \beta \|\mathbf{L}\|_{RTV} + \lambda \|\mathbf{I}\|_{1} + \gamma \|\mathbf{G}\|_{F}^{2},$$

$$s.t. \quad \mathbf{L} + \mathbf{G} + \mathbf{I} = \mathbf{Y}$$
(8)

where  $\alpha$ ,  $\beta$ ,  $\lambda$ , and  $\gamma$  are regularization coefficients;  $\|\mathbf{L}\|_{w.s_p}^p$  is the Schatten p-norm term; and  $\|\mathbf{L}\|_{RTV}$  is the smoothness preservation term (which includes the prior sparsity information of the images); the three-term  $\|\mathbf{I}\|_1$  is the L<sub>1</sub> norm and the sparsity regularization term and is used as the fidelity term of impulse noise; and  $\|\mathbf{G}\|_F^2$  is the Frobenius norm, which is used as the fidelity term of Gaussian noise.

#### 3.4. SOLUTION FOR RTV-WSPM WITH ADMM

The variable splitting method is employed to solve RTV-WSPM. By introducing an augmented variable (**Z**), the RTV-WSPM model can be reformulated as a linear equality-constrained problem with two variables (**L** and **Z**). Eq. (8) can be solved under the ADMM [7] framework. The augmented Lagrangian function is as follows:

$$\underset{\mathbf{L},\mathbf{Z},\mathbf{I},\mathbf{G}}{\operatorname{arg min}} \alpha \|\mathbf{L}\|_{w,S_{p}}^{p} + \beta \|\mathbf{Z}\|_{RTV} + \lambda \|\mathbf{I}\|_{1} + \gamma \|\mathbf{G}\|_{F}^{2},$$

$$s.t. \quad \mathbf{L} + \mathbf{G} + \mathbf{I} = \mathbf{Y} \cdot \mathbf{L} = \mathbf{Z}$$
(9)

As the four variables (**L**, **Z**, **I**, **G**) of Eq. (9) are independent, the augmented Lagrange multiplier (ALM) [7] is applied to relax the equality constraints of (9), and the following function is obtained as the following:

$$\mathbf{M}_{\rho}(\mathbf{L}, \mathbf{Z}, \mathbf{I}, \mathbf{G}; \mathbf{W}, \mathfrak{I}) = \alpha \|\mathbf{L}\|_{\omega, s_{\rho}}^{p} + \beta \|\mathbf{Z}\|_{RT^{p}} + \lambda \|\mathbf{I}\|_{1} + \gamma \|\mathbf{G}\|_{F}^{2} + \frac{\rho}{2} \left\|\mathbf{L} + \mathbf{G} + \mathbf{I} - \mathbf{Y} + \frac{\mathbf{W}}{\rho}\right\|_{2}^{2} + \left\|\mathbf{L} - \mathbf{Z} + \frac{\mathfrak{I}}{\rho}\right\|_{2}^{2}\right), (10)$$

where **W** is the Lagrange multiplier matrix associated with constraint  $\mathbf{L} + \mathbf{G} + \mathbf{I} = \mathbf{Y}$ ,  $\Im$  is the Lagrange multiplier matrix associated with constraint  $\mathbf{L} = \mathbf{Z}$ , and  $\mathcal{P}$  is a positive scalar.

Subsequently, the general framework of the ADMM is used to solve Eq. (10) by the following iterative scheme.

(1) Update L at the (k+1)th iteration and fix other variables, except for L in Eq. (10) to obtain the following sub-problem:

$$\mathbf{L}_{k+1} = \mathop{\arg\min}_{\mathbf{L}} \mathsf{M}_{\rho}(\mathbf{L}, \mathbf{Z}_k, \mathbf{I}_k, \mathbf{G}_k; \mathbf{W}_k, \mathfrak{I}_k) = \mathop{\arg\min}_{\mathbf{L}} \frac{\alpha}{\rho_k} \left\| \mathbf{L} \right\|_{w, s_p}^p + \frac{1}{2} \left\| \mathbf{L} - \mathbf{D}_k \right\|_F^2, (11)$$

$$\begin{aligned} \mathbf{D}_k &= \frac{1}{2} (\mathbf{Y} + \mathbf{Z}_k - \mathbf{I}_k - \mathbf{G}_k) - \frac{(\mathbf{W}_k + \mathfrak{T}_k)}{\rho_k} &\text{. By ordering} \\ \mathbf{D}_k &= U \mathrm{diag}(\sigma_1, \sigma_2, ... \sigma_r) V^T \text{, the optimal solution of Eq. (11) will} \\ \mathrm{be} & \ \mathbf{L}_{k+1} &= \mathbf{U}_k \Delta \mathbf{V}_k^\mathrm{T} \text{ with } \Delta = diag(\delta_1, \delta_2, ... \delta_r) \text{, where } \delta_i \text{ is given} \\ \mathrm{by generalized soft-thresholding [5]}. \end{aligned}$$

(2) Update **Z** for spatial smoothness preservation and fix other variables, except for **Z** in Eq. (10), to obtain the following sub-problem:

$$\mathbf{Z}_{k+1} = \arg\min_{\mathbf{Z}} \frac{\beta}{\rho_k} \|\mathbf{Z}\|_{RTV} + \frac{1}{2} \|\mathbf{Z} - \mathbf{T}_k\|_F^2, \tag{12}$$

where  $\mathbf{T}_k = \mathbf{L}_k + \mathfrak{T}_k / \rho_k$ . Many efforts have been made to develop efficient and scalable algorithms for the TV problem. Here, we adopt the fast gradient based algorithm [18] to solve the subproblem (Eq.(12)).

(3) Update I for impulse noise removal and fix other variables, except for I in Eq. (10), to obtain the following sub-problem:

$$\mathbf{I}_{k+1} = \arg\min_{\mathbf{Z}} \frac{\lambda}{\rho_k} \|\mathbf{I}\|_1 + \frac{1}{2} \|\mathbf{I} - \mathbf{E}_k\|_F^2, \tag{13}$$

where  $\mathbf{E}_k = \mathbf{Y} - \mathbf{L}_{k+1} - \mathbf{G}_k - \mathbf{W}_{k/\rho_k}^{\mathsf{v}}$ . Thereafter, the closed form solution of Eq. (13) can be obtained by resorting to the elementwise shrinkage operator, that is,  $\mathbf{I}_{k+1} = sign(\mathbf{E}_k) \max\{|\mathbf{E}_k| - \frac{\imath}{2}\rho_k, 0\}$ .

(4) Update **G** for Gaussian noise removal and fix other variables, except for **G** in Eq. (10), to obtain the following sub-problem:

$$\mathbf{G}_{k+1} = \underset{\mathbf{G}}{\operatorname{arg\,min}} \, \gamma \left\| \mathbf{G} \right\|_F^2 + \frac{\rho_k}{2} \left\| \mathbf{G} - \mathbf{S}_k \right\|_F^2, \tag{14}$$

where  $\mathbf{S}_k = \mathbf{Y} - \mathbf{L}_{k+1} - \mathbf{I}_{k+1} - \mathbf{W}_{k}$ . This outcome is a standard

least squares regression problem, and the closed-form solution is  $\mathbf{G}_{k+1} = (2 \times \gamma + \rho_k)^{-1} \rho_k \mathbf{S}_k$ .

(5) Update **W** and  $\mathfrak{T}$  using the following equations:

$$\begin{cases}
\mathbf{W}_{k+1} = \mathbf{W}_{k} + \rho_{k} (\mathbf{L}_{k+1} + \mathbf{G}_{k+1} + \mathbf{I}_{k+1} - \mathbf{Y}) \\
\mathbf{\mathfrak{I}}_{k+1} = \mathbf{\mathfrak{I}}_{k} + \rho_{k} (\mathbf{L}_{k+1} - \mathbf{Z}_{k+1}) \\
\rho_{k+1} = \min\{\mu \times \rho_{k}, \rho_{\max}\}
\end{cases} (15)$$

where  $\mu > 1$  is a shrinkage factor for facilitating further the convergence speed and  $\rho_{\max}$  is the maximum value of  $\rho$ .

#### 3.5. RTV-WSPM FOR IMAGE DENOISING

The nonlocal similar patches of observation data y in a large enough local window are searched by methods such as the Knearest neighbor. By stacking those nonlocal similar patches into a matrix and denoting by  $\mathbf{Y}_{i}$ , we have  $\mathbf{Y}_{i} = \mathbf{L}_{i} + \mathbf{S}_{i} + \mathbf{N}_{p}$ , where  $\mathbf{L}_{p} \cdot \mathbf{S}_{p}$ , and  $\mathbf{N}_{i}$  are the patch matrices of the original image, impulse noise, and Gaussian noise, respectively.

Algorithm 1 provides the details of the proposed RTV-WSPM operator for each  $\mathbf{Y}_i$  to estimate  $\mathbf{L}_i$  for image denoising. Algorithm 2 summarizes the proposed algorithm of RTV-WSPM for the whole image denoising.

#### Algorithm 1 RTV-WSPM operator for each Y, to estimate L,

Input: Noisy image Y,

1: Initialize:  $\mathbf{L} = \mathbf{Z} = \mathbf{I} = \mathbf{G} = \mathbf{W} = \mathfrak{I} = 0$ ,  $\varepsilon = 10^{-7}$ , t=0, and p=0.6

2: while not converged do

3: Apply the RTV-WSPM operator to Y, to estimate L, Update

 $\mathbf{L}_{k+1}$ ,  $\mathbf{Z}_{k+1}$ ,  $\mathbf{I}_{k+1}$ ,  $\mathbf{G}_{k+1}$ ,  $\mathbf{W}_{k+1}$ ,  $\mathfrak{F}_{k+1}$  by (11), (12), (13), (14), and (15), respectively;

4: Check the convergence conditions

5: end while

Output: Denoised image L.

#### Algorithm 2 Image denoising via RTV-WSPM

**Input**: Noisy image y

1: Initialize  $I^{(0)} = V$ ;  $V^{(0)} = V$ 

2: for k=1:*K* do

3: Iterative regularization  $y^{(k)} = I^{(k-1)} + \delta(y - y^{(k-1)})$ 

4: for each patch  $\mathbf{Y}$  in  $\mathbf{v}^{(k)}$  do

5: Find similar patch group Y.

6: Apply **Algorithm** 1 to  $\mathbf{Y}_i$  to estimate  $\mathbf{L}_i$ 

7: end for

8: Aggregate  $\mathbf{L}_i$  to form the clean image  $I^{(k)}$ 

9: end for

Output: Denoised image L(K)

#### 4. RESULT ANALYSIS AND DISCUSSION

In this section, the proposed RTV-WSPM-based image denoising algorithm was compared with several state-of-the-art denoising methods, including BM3D [2], WNNM [5], RM [8], and WSNM [9]. The baseline NNM algorithm was also compared. All the competing methods employ the image non-local redundancies. Aside

from visual quality, we also employed two quantitative quality indexes—the peak signal-to-noise ratio (PSNR) and feature structural similarity (FSIM)—to measure the reconstruction accuracies. The PSNR and FSIM are defined in Eq. (16) and (17).

$$PSNR = 10 \lg \frac{(\text{Max}(f, f))^{2}}{\|f - f\|_{F}^{2}}$$
 (16)

where f denotes the original image and f is the restored image,  ${\rm Max}(f,f)$  represents the maximum function.

FSIM is defined as

$$FSIM = \frac{\sum_{z \in \Omega} G(z) * PC(z)}{\sum_{z \in \Omega} PC(z)}$$
(17)

where G(z) is the gradient magnitude for the position z, PC(z) denotes phase congruency for position z of image I and  $\Omega$  is the whole image spatial domain.

Noisy MRI images, 50 natural images from the Berkeley (BSD200) datasets, and 20 images of different sizes from the USC-SIPI image database were selected for quantitative assessment. All the experiments were run in MATLAB 2015a on a 64-bit personal computer with an Intel(R) Core(TM) i5-2520M CPU @ 2.5GHz CPU and 8 GB memory.

The proposed algorithm has several parameters. For all noise levels, iterative regularization parameter  $\delta$  and parameter p were fixed to 0.1 and 0.8, respectively. Iteration number K and patch number p were set on the basis of the noise level. By experience,

we set the patch size to 7 × 7. K was set to 8, and g was set to 80. The  $\alpha$ ,  $\beta$ ,  $\lambda$ ,  $\gamma$ ,  $\mu$ , and  $\rho$  of the RTV-WPSM model are 0.1, 0.005, 0.002, 0.87, 10<sup>-6</sup>, and 1.1, respectively. The source codes of the competing methods were obtained from the original authors, and we used the default parameters.

## 4.1 EXPERIMENTAL RESULTS ON NOISY MR IMAGES AND 50 TEST IMAGES

We initially demonstrated the effectiveness of the proposed RTV-WSPM method for white Gaussian additive noise removal. The Gaussian white noises with standard deviations of 30, 40, 50, 60, and 70 were added to the test images as the noisy observations to quantitatively evaluate the performance of the proposed method.

Fig. 1 depicts the PSNR and FSIM average results of the proposed RTV-WSPM denoising method compared with the competing denoising techniques of BM3D, WNNM, RM, and WSPM.

The proposed RTV-WSPM and WSNM achieve the highest PSNR values in all cases (Fig. 1). Moreover, the proposed RTV-WSPM, BM3D, and WSNM outperform the RM and WNNM (Fig. 1[a]) using the noise with standard deviations of 30, 40, and 50. As RM adopts hard threshold shrinkage, image structure information is lost quickly as noise with the increase of standard deviation. Clearly, the proposed method enjoys evident gain over the four competing anchors on average at different noise levels (Fig. 1[b]) by the average value of FSIM. Thus, the structure information of the image can be well retained by adding RTV regularization. Conversely, the probability of losing the image structure with a low-rank structure of matrix forms a similarity image block that can be effectively reduced to improve the denoising performance.

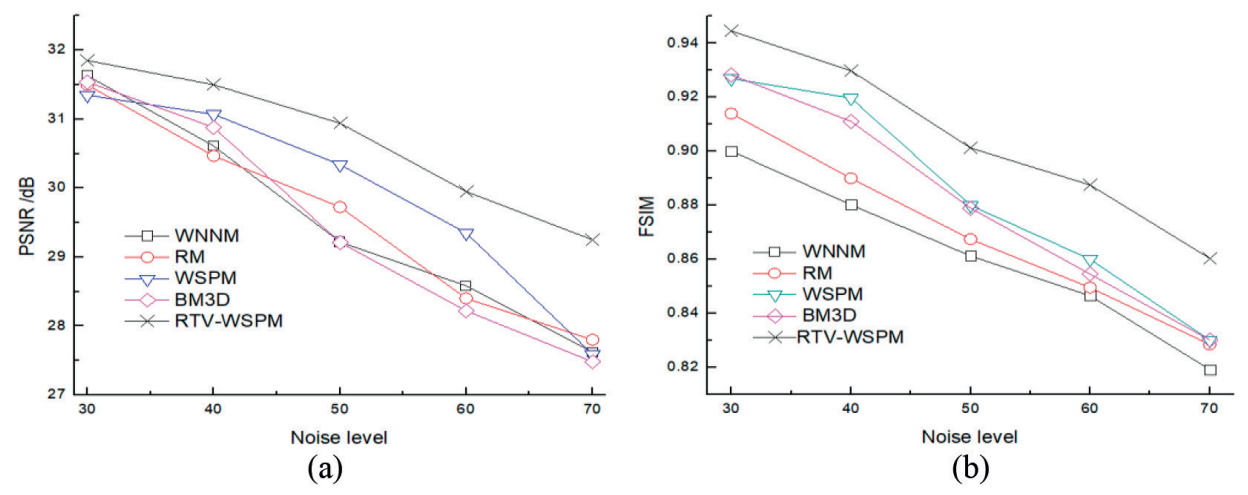


Fig. 1: Comparison of the PSNR and FSIM results of different methods for image denoising on 50 images from Berkeley. (a) PSNR values and (b) FSIM values

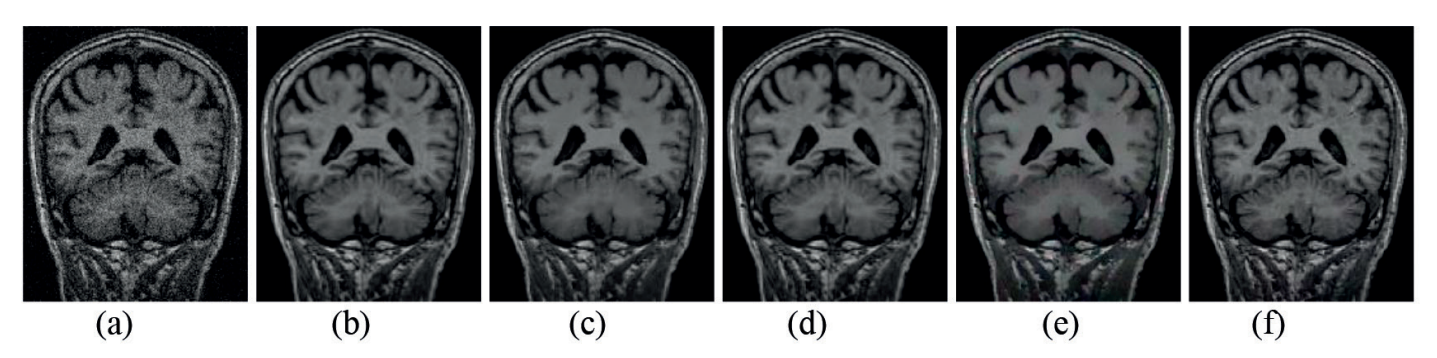


Fig. 2: Denoising results on brain MRI images with noise. From left to right: (a) noisy input ( $\sigma$ = 35), (b) RM, (c) BM3D, (d) WSPM, (e) WNNM, and (f) the proposed RTV-WSPM

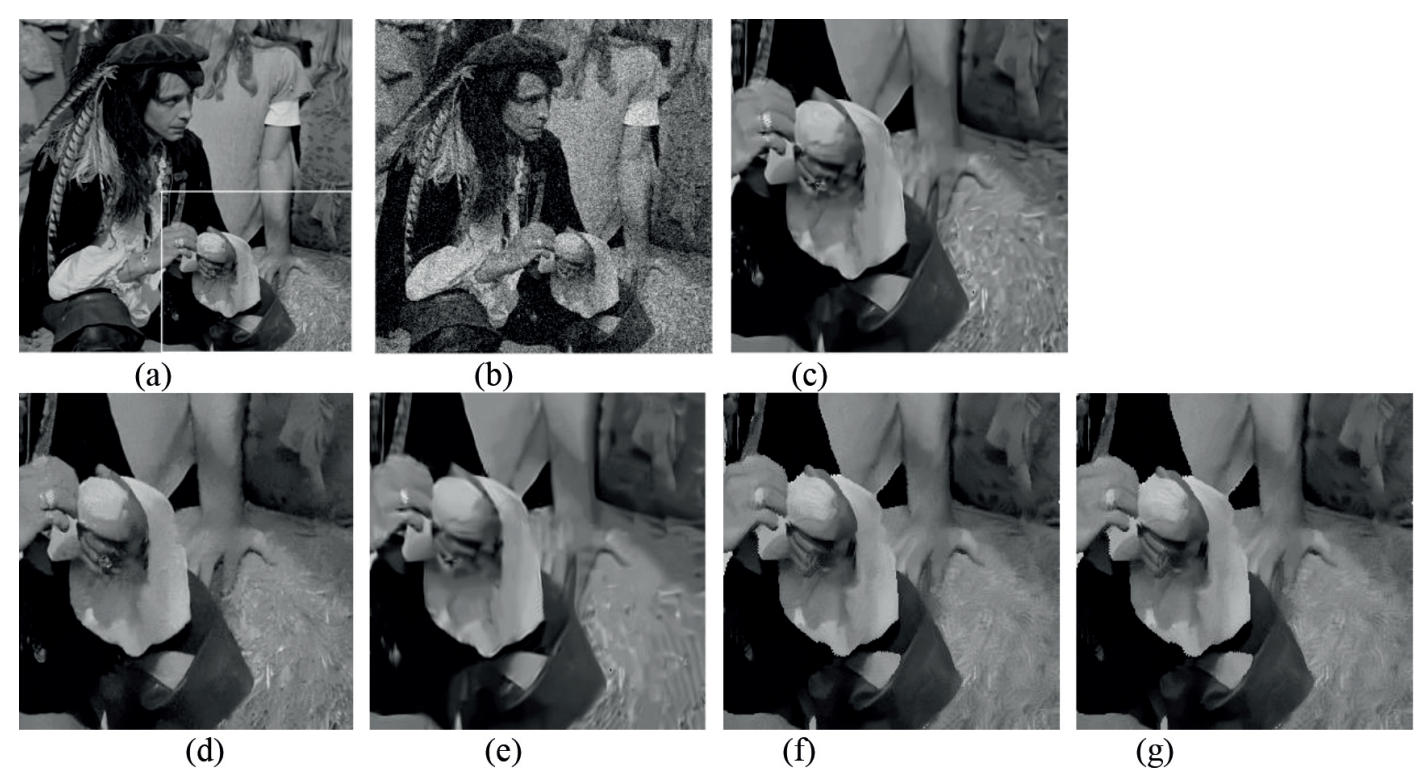


Fig. 3: Fragments of restoration results on a male image by different methods (noise level 30%); (a) original image, (b) noisy image, (c) proposed RTV-WSPM, (d) WNNM, (e) WSPM, (f) BM3D, and (g) RM. The patch in white window represents the part patch. (c)–(g) are the details of the restoration results for the patch in the white window

Fig. 2 depicts the comparison of the denoising of brain MRI images with noise. The core part of the brain for denoising is fuzzy with the RM and WNNM algorithms (Fig. 2). More importantly, the proposed method produces the restored images of good perceptual quality. The output of Fig. 2(f) are evidently clearer, have several details, and show few artifacts. Such image is more helpful for auxiliary medical diagnosis.

### 4.2. EXPERIMENTAL RESULTS ON 20 TEST IMAGES WITH SALT-AND-PEPPER NOISE

In this subsection, we aim to test the salt-and-pepper noise removal on 20 test images from the USC-SIPI image database. The fragments of restoration results on the male image (Fig. 3)

shows the visual comparison of all methods. Clearly, our proposed RTV-WSPM achieves higher perceptual quality, meaning that RTV-WSPM outperforms other competing methods for salt-and-pepper noise removal.

The lawn texture details of Fig. 3(c) are clear and well preserved by the proposed RTV-WSPM denoising method, whereas the other methods have serious ambiguities in the ground texture of the denoising details (Figs. 3[d]–[g]).

Table 1 lists the average PSNR and FSIM results of all denoising methods on four testing images (boat, male, peppers, and Pentagon). Our proposed RTV-WSPM achieves the highest PSNR values in almost cases. RTV-WSPM outperforms the best competing methods at least 0.86 dB and 0.102, respectively. Our proposed

τ	Image	Proposed	WNNM	RM	WSNM	ВМЗД
0.2	Boat	32.29/0.943	31.37/0.913	31.23/0.901	31.68/0.912	31.58/0.911
	Male	31.79/ <u><b>0.939</b></u>	31.53/0.910	31.19/0.907	31.25/0.921	<b>31.90</b> /0.919
	Peppers	<b>32.23</b> /0.901	31.08/0.889	31.25/0.892	31.89/0. 917	31.85/ <u><b>0. 922</b></u>
	Pentagon	31.95/ <u><b>0.921</b></u>	31.28/0.901	31.75/0.863	31.47/0.902	<b>31.90</b> /0.910
0.3	Boat	<u>30.99/</u> 0.833	28.98/0.827	28.86/0.842	29.19/ <b>0.848</b>	28.74/0.842
	Male	30.65/0.894	28.58/0.821	27.96/0.829	28.81/0.859	28.52/0.831
	Peppers	30.58/0.887	28.71/0.841	27.89/0.819	28.76/0.812	28.54/0.827
	Pentagon	30.42/0.893	28.63/0.830	27.94/0.853	28.68/0.805	28.72/0.841
0.4	Boat	28.22/0.821	27.13/0.712	26.31/0.703	27.35/0.745	27.10/0.727
	Male	28.16/0.837	26.78/0.704	26.20/0.651	27.46/0.760	27.02/0.704
	Peppers	28.44/0.803	26.22/0.692	26.16/0.609	27.30/0.725	26.52/0.687
	Pentagon	28.68/0.819	26.42/0.699	26.05/0.608	27.27/0.713	26.32/0.647

Table 1: Quantitative comparison of the denoised results of different methods in terms of PSNR and FSIM with different noise levels

RTV-WSPM reconstructed images with noise by ratio  $\tau$  from 0.2 to 0.4 and achieved higher PSNR and SSIM values in all cases over other competing methods. Therefore, the RTV-WSPM is more robust to the changes of the ratios of impulse noise on the 20 test images than the other competing methods.

#### 5. CONCLUSION

To enhance the image structure retention of the WSPM algorithm, the RTV-WSPM, a weighted Schatten p-norm minimization with RTV regularization, is proposed in this study to minimize the over-smoothing from denoising. The experiments reveal that our proposed method outperforms other techniques. Thus, several observations can be drawn:

- (1) For the image denoising with a salt-and-pepper noise task, low-rank approximations with TV regularization-based approaches outperform other approximation-based approaches.
- (2) The comparison of PSNR and FSIM and visual effects indicates that RTV-WSPM is applicable for a variety of noises, including Gaussian, salt-and-pepper, and mixed noise. This capability is mainly due to the fact that our model exploits the RTV relationships in the local window and local spatial smoothness.

Since RTV-WSPM need calculation low rank by SVD, the time complexity of the algorithm is too difficult to apply the practical application. Therefore, several directions may be considered in future work. Developing fast and scalable parallel computing algorithms for our proposed model should be considered. One potential scheme is to utilize an optimization technique that considerably reduces the calculation to capture the low-rank property.

#### **REFERENCES**

- [1] LUO Xuegang, LV Junrui, WANG Huajun, et al. "Fast Nonlocal Means Image Denoising Algorithm Using Selective Calculation". Journal of University of Electronic Science and Technology of China, January 2015. Vol.44-1. p.84-90. DOI:http://dx.chinadoi.cn/10.3969/j.issn.1001-0548.2015.01.014
- [2] DABOV K, FOI A, KATKOVNIK K O, et al. "Image denoising by Sparse 3D transform domain collaborayive filtering". IEEE Transactions on Image Proscessing, August 2007. Vol.16-8. p.2080-2095. DOI: https://doi.org/10.1109/tip.2007.901238
- [3] Gu S, Xie Q, Meng D, et al. "Weighted Nuclear Norm Minimization and Its Applications to Low Level Vision". International Journal of Computer Vision, January 2017. Vol.121–2. p.183–208. DOI: https://doi.org/10.1007/s11263-016-0930-5
- [4] Xie Y, Gu S, Liu Y, et al. "Weighted Schatten p-norm minimization for image denoising and background subtraction". IEEE transactions on image processing, October 2016. Vol.25-10. p. 4842-4857. DOI: https://doi. org/10.1109/tip.2016.2599290
- [5] Liu L, Huang W, Chen D, et al. Exact minimum rank approximation via Schatten p-norm minimization[J]. Journal of Computational and Applied Mathematics, September 2014. Vol.267-1. p.218-227. DOI: https://doi. org/10.1016/j.cam.2014.02.015
- [6] W. Dong, G. Shi, and X. Li, "Nonlocal image restoration with bilateral variance estimation: a low-rank approach", IEEE Transactions on Image Processing, February 2013 Vol.22-2. p.700-711. DOI: https://doi.org/10.1109/ tip.2012.2221729
- [7] S. Gu, L. Zhang, W. Zuo, and X. Feng. "Weighted nuclear norm minimization with application to image denoising". IEEE Conference on Computer Vision and Pattern Recognition, June 2014. p.2862–2869. DOI: https://doi. org/10.1109/cvpr.2014.366
- [8] K. Hosono, S. Ono, and T. Miyata, "Weighted tensor nuclear norm minimization for color image denoising". IEEE International Conference on Image Processing. September 2016. p.3081–3085. DOI: https://doi.org/10.1109/ icip.2016.7532926

- [9] Huang Y , Yan H , Wen Y , et al. "Rank minimization with applications to image noise removal". Information Sciences, March 2018. Vol.429-6. p.147-163. DOI: https://doi.org/10.1016/j.ins.2017.10.047
- [10]M. Signoretto, R. Van de Plas, B. De Moor et al. "Tensor versus matrix completion: A comparison with application to spectral data". IEEE Signal Processing Letters. July 2011. Vol.18-7. p.403-406. DOI: https://doi. org/10.1109/lsp.2011.2151856
- [11] Feng Zhenjie, Han Weixue . "Seismic signals blind denoising based on W weighted nuclear norm minimization". Laser & Optoelectronics Progress, April 2019. Vol.56-7:071503. DOI: http://dx.doi.org/10.3788/lop56.071503
- [12] Cai J F , Candès, Emmanuel J, et al. "On Accelerated Singular Value Thresholding Algorithm for Matrix Completion". SIAM Journal on Optimization, December 2014. Vol.5-21. p.3445-3451. DOI: https://doi. org/10.4236/am.2014.521322
- [13] Hu Y, Zhang D, Ye J, et al. "Fast and accurate matrix completion via truncated nuclear norm regularization". IEEE transactions on pattern analysis and machine intelligence, 2013, 35(9): 2117–2130. DOI: https://doi.org/10.1109/tpami.2012.271
- [14] K. Mohan and M. Fazel. "Iterative reweighted least squares for matrix rank minimization". 48th Annual Allerton Conference on Communication, Control, and Computing. September 2010. Vol. 13-1. p. 3441–3473, 2010. DOI: https://doi.org/10.1109/allerton.2010.5706969
- [15] A. Eriksson and A. van den Hengel, "Efficient computation of robust lowrank matrix approximations in the presence of missing data using the L1 norm". IEEE Computer Society Conference on Computer Vision and Pattern Recognition. June 2010. p.771–778. DOI: https://doi.org/10.1109/ cvpr.2010.5540139
- [16] P. Chatterjee and P. Milanfar, "Patch-based near-optimal image denoising". IEEE Transactions on Image Processing. April 2012. Vol. 21-4. p. 1635–1649. DOI: https://doi.org/10.1109/tip.2011.2172799
- [17] LIU S J, WU G Q, ZHANG X Z, et al. "SAR Image denoising via linear minimum mean square error estimation". Systems Engineering and Electronics. April 2016. Vol.38-4. p.785-791. DOI: http://dx.chinadoi.cn/10.3969/j.issn.1001-506X.2016.04.10
- [18] FENG X, LI K X, YU W J, et al. "Fast matrix completion algorithm based on randomized singular value decomposition and its applications". Journal of Computer-Aided Design and Computer Graphics. December 2017. Vol.29-12. p. 2343-2348. DOI: https://doi.org/10.3724/sp.j.1089.2017.16603
- [19] ZHANG W Q, ZHANG H Z, ZUO W M, etal. "Weighted nuclear norm minimization model for matrix completion". Computer Science. July 2015. Vol.42-7. p.254-257. DOI: http://dx.chinadoi.cn/10.11896/j.issn.1002-137X.2015.07.054
- [20] Beck A, Teboulle M. "Fast Gradient-Based Algorithms for Constrained Total Variation Image Denoising and Deblurring Problems". IEEE Transactions on Image Proscessing, November 2009. Vol.18-11. p.2419-2434. DOI: https://doi.org/10.1109/tip.2009.2028250
- [21] Xu L, Yan Q, Xia Y, et al. "Structure extraction from texture via relative total variation". ACM Transactions on Graphics. November 2012. Vol.31-6. p.439-445. DOI: https://doi.org/10.1145/2366145.2366158
- [22] L. Zhang, L. Zhang, X. Mou, et al. "FSIM: A feature similarity index for image quality assessment". IEEE Transactions on Image Processing. August 2011. Vol.20-8. p.2378–2386. DOI: https://doi.org/10.1109/tip.2011.2109730

#### **APPRECIATION**

This research was funded by Natural Science Foundation of Sichuan Province of China under Grant No. 2019YJ0342 and Innovation Foundation(Believe in Engineering) of Sichuan Province of China under Grant No.2019088.